Available online at www.sciencedirect.com
ScienceDirect
Journal of Photochemistry and Photobiology A: Chemistry 193 (2008) 260–265
Journal of Photochemistry and Photobiology A:Chemistry
www.elsevier.com/locate/jphotochem

Medium effects on the fluorescence spectra of tertiary aliphatic amines in mixed solvents and supercritical fluids

Tsuguyoshi Toyooka [a], Shinsuke Ohchi [a], Yoshimi Sueishi [a], Shunzo Yamamoto [a,*], Okitsugu Kajimoto [b]

[a] *The Graduate School of Natural Science and Technology, Okayama University, 3-1-1 Tsushimanaka, Okayama 700-8530, Japan*
[b] *Department of Chemistry, Graduate School of Science, Kyoto University, Kitashirakawa-Oiwakecho, Sakyo-ku, Kyoto 606-8502, Japan*

Received 22 May 2007; received in revised form 26 June 2007; accepted 5 July 2007
Available online 10 July 2007

Abstract

Emission spectra of some tertiary amines were measured in cyclohexane (CH)–tetrahydrofuran (THF) mixtures and in supercritical fluids of CHF_3. The emission bands of these amines were found to show large successive red shifts with increasing concentration of polar solvent molecules. This finding was rationalized by considering the consecutive solvation of the polar molecules around the Rydberg excited state of the amine. In order to estimate the degree of solvation, the wavenumbers of the emission maxima were plotted as functions of the THF and CHF_3 concentrations. The changes in solvation number with increasing THF and CHF_3 concentrations were obtained from the spectral shifts by applying a calculation for the stepwise solvation model.
© 2007 Elsevier B.V. All rights reserved.

Keywords: Medium effect; Fluorescence spectra; Tertiary amines; Supercritical fluid; Mixed solvent; Stepwise solvation model

1. Introduction

Saturated tertiary amines are the most remarkable examples of aliphatic molecules exhibiting strong fluorescence emission in the vapor phase [1–3], as well as in solution [4,5]. The fluorescence quantum efficiencies of saturated tertiary amines in the vapor phase and in nonpolar solvents have been shown to be quite large. The amines are strongly emissive also in saturated ethers. There are large red shifts in the emission spectra of the tertiary amines in ethers relative to nonpolar solvents. The overall red shift upon going from cyclohexane (CH) ($\lambda_{max} = 285$ nm) to tetrahydrofuran (THF) ($\lambda_{max} = 344$ nm) is large.

Excitation of tertiary amines leads to Rydberg-type excited states characterized by an excited orbital of large spatial extension [6,7]. Such states are assumed to undergo strong perturbations resulting from interactions with the surrounding molecules, and this is demonstrated by efficient fluorescence quenching in polar solvents [8,9].

Muto et al. [8] observed large red shifts in the emission spectrum of 1,4-diaza-bicyclo[2,2,2]octane (DABCO) in ether solvents relative to nonpolar solvents. Similar large red shifts in the emission spectra of triethylamine (TEA) and *N*,*N*-diethylmethylamine (DEMA) in similar solvents were reported by van der Auweraer et al. [10] and Halpern [11]. Muto et al. explained the observation by the stabilization of the excited state of the amine by the ether solvents using the model of a solvated Rydberg state. Halpern also discussed the red shift in the emission spectrum of DEMA within the framework of universal and specific interactions between the excited amine and ether molecules, and discussed the exciplex formation. However, no evidence for the formation of intra and intermolecular 1:1 amine–ether exciplexes was found. He concluded that the original view of Muto et al. may account satisfactorily for the observation, though the possibility of the formation of higher associates remains [11].

Halpern et al. investigated the structural effects on photophysical processes and excimer formation in saturated amines [3,12,13], and also examined the fluorescence properties of members of the series ($(CH_3)_2N$–$(CH_2)_n$–$N(CH_3)_2$) and observed emission from excited monomer and an intramolecular

* Corresponding author.
E-mail address: yamashun@cc.okayama-u.ac.jp (S. Yamamoto).

1010-6030/$ – see front matter © 2007 Elsevier B.V. All rights reserved.
doi:10.1016/j.jphotochem.2007.07.004

excimer for $n = 3$ and 4 [14]. We observed broad and asymmetric emission spectra with some saturated diamines which have a primary and a tertiary amino group. These spectra were resolved into three component bands, and they were assigned to excited tertiary and primary amino group moieties and an intramolecular exciplex between an excited tertiary amino group and a ground state primary amino group [15,16].

Kohler studied the steady state and time-resolved fluorescence spectroscopy of triethylamine–ethanol and –deuterated ethanol mixtures and observed exciplex formation at low alcohol concentrations in hydrocarbon solution [17–19].

In amine–amine and amine–alcohol systems, the formation of excimer and exciplex was observed. As mentioned above, however, in amine–ether system the specific interaction between the excited amine and ether molecules was not observed.

Shang et al. studied solvent induced singlet (2p3s) Rydberg relaxation dynamics of DABCO in van der Waals clusters generated in a supersonic expansion. The singlet Rydberg state dynamics were found to depend upon cluster geometry, cluster size, and cluster vibrational energy. These results suggested that the Rydberg state is reactive and susceptible to environmental perturbation [20].

The examination of the dependence of the emission spectrum on the composition of the polar solvent in nonpolar–polar mixed solvents or that on the density of supercritical fluids of polar species can give more detailed information about the solvation of the excited tertiary amines. Solvation of polar solvent molecules is expected to occur stepwise by increasing the content of the polar solvent in CH–THF mixtures or by increasing the density in supercritical fluids of CHF_3.

In this study, the effects of the stepwise solvation of THF and CHF_3 molecules on the emission spectra of different types of tertiary amines have been examined in the CH–THF mixtures and in supercritical fluids of CHF_3.

2. Experimental

All the reagents were obtained from commercial sources. TEA (extra pure grade) was used after drying with potassium hydroxide and a trap-to-trap distillation. 1-Azabicyclo [2,2,2]octane (ABCO) was used as supplied. Trioctylamine (TOA) was used after drying with potassium hydroxide and filtration. CH, THF and diethyl ether (DEE) were of spectroscopic grade and were used as available. Diisopropyl ether (DIPE; extra pure grade) was used after drying with calcium hydride and distillation. CHF_3 gas was of high-purity.

The steady-state fluorescence spectra of amines in CH, THF, DEE, DIPE and CH–THF mixtures were measured by using a Shimadzu spectrofluorophotometer, model RF-5300PC (band pass typically 10 nm) at room temperature. The concentrations of amines were 3.0×10^{-4} mol dm^{-3}. The solutions were degassed by four freeze–pump–thaw cycles immediately prior to measurement. Excitation was effected at 245 nm in each case.

The optical cell for the supercritical fluid experiments was made of stainless steel (SUS 304) with three quartz windows of 15 mm diameter. The cell was evacuated and sample gases were introduced using a vacuum line. Supercritical CHF_3 was fed to the cell with an HPLC pump (JASCO, SCF-Get). The pressure in the cell was changed by adding CHF_3 successively, and the pressure was monitored with a strain pressure gauge (Kyowa, PGM-200KH). The temperature of the cell was monitored with a K-type thermocouple and maintained at 35.0 ± 0.2 °C by circulating hot water from the thermostated water bath (Tokyo Rika Co. UA-100G) through the cell. The fluorescence spectra of TEA and ABCO in supercritical CHF_3 were obtained with a Shimadzu spectrofluorophotometer, model RF-5300PC) using the high-pressure cell. The pressure was monitored with a piezo gauge and the density was calculated from the P-V-T data for CHF_3 [21].

3. Results and discussion

According to the model postulated by Muto et al. the stabilization energy (ΔE) of the excited amine was expressed approximately as follows:

$$\Delta E = E_{ex} - E_{ep} - E_{op} \quad (1)$$

where E_{ex} is a repulsive exchange energy between the Rydberg electron and solvent molecules, and E_{ep} and E_{op} are electronic and orientational polarization energies, respectively. They estimated the quantity ($E_{ex} - E_{ep}$) from the energy of blue shift of the Rydberg absorption band, and E_{op} from the ion–dipole interaction energy. They could obtain an explanation for the observation of a shift of the emission band of DABCO by using a model in which several polar solvent molecules are solvated to the Rydberg state of the amine.

In order to examine the solvent polarity dependence of the emission band using the successive solvation model in more detail, the emission spectra of TEA were measured in CH, THF and several CH–THF mixtures. The results are shown in Fig. 1. The observed spectra show large successive bathochromic shifts with increasing THF content. Similar spectral shifts in CH–THF mixtures were observed for ABCO and TOA. Fig. 2 shows the wavenumbers of the emission peak of TEA as a function of the relative permittivity of CH–THF mixtures and some neat solvents. As shown in Fig. 2, the shifts of the emission band in

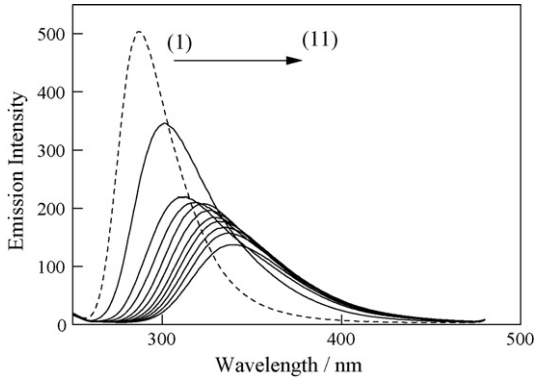

Fig. 1. Emission spectra of TEA in CH/THF mixtures with different concentrations of THF. (1) [THF] = 0 mol dm^{-3}, (2) 1.23 mol dm^{-3}, (3) 2.47 mol dm^{-3}, (4) 3.70 mol dm^{-3}, (5) 4.93 mol dm^{-3}, (6) 6.17 mol dm^{-3}, (7) 7.40 mol dm^{-3}, (8) 8.63 mol dm^{-3}, (9) 9.86 mol dm^{-3}, (10) 11.10 mol dm^{-3} and (11) 12.33 mol dm^{-3}.

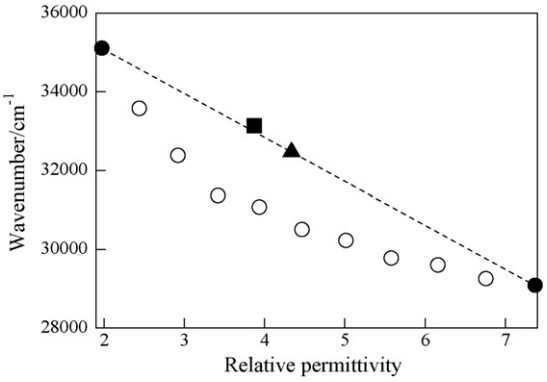

Fig. 2. The wavenumbers of the emission maximum of TEA against relative permittivity in CH, DEE, DIPE, THF, and CH/THF mixtures with different concentration of THF: (●) CH and THF; (■) DIPE; (▲) DEE; (◯) CH/THF.

CH–THF mixtures are larger than those in neat solvents having similar relative permittivities. This shows that the preferential solvation of THF occurred in CH–THF mixtures.

In neat CH, TEA shows an emission band with a maximum at 285 nm. As the composition of THF increases, the position of the emission maximum moves toward longer wavelengths. Fig. 3 shows the wavenumbers of the emission maxima of TEA against the concentration of THF in CH–THF mixtures.

Although TOA has much larger alkyl groups than TEA, the shift of emission band for TOA was very similar to that for TEA. This indicates that the solvation model in which solvent molecules associate successively around the sphere accommodating a solute molecule does not work in the present case. In order to explain the similarity of the solvent effects on emission bands for TOA and TEA, we proposed the model shown in Fig. 4. In this model, polar solvent molecules associate between alkyl groups above and below the planar excited amine molecule and the attachment of solvent molecules are not appreciably affected by the bulkiness of alkyl groups.

By the successive solvation model proposed by Kajimoto et al. [22,23], the following equation can be obtained (see Appendix A):

$$C_m = C_1 \frac{m(n-1)}{n-m} \tag{2}$$

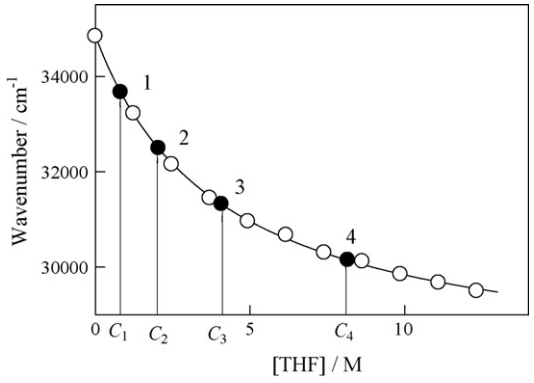

Fig. 3. The wavenumbers of the emission maxima of TEA against the concentration of THF in CH/THF mixtures: (◯) observed shifts; (●) calculated shifts from Eq. (2) (see text) (solvation numbers are shown along the curve).

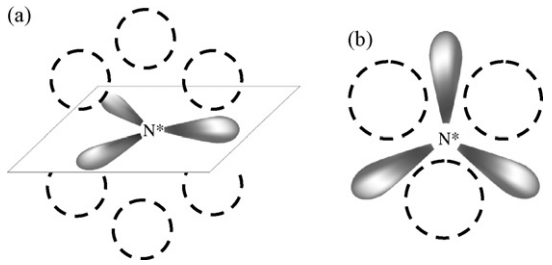

Fig. 4. A schematic model of solvated Rydberg states of TEA and TOA. Polar solvent molecules are illustrated as cubes (a) and top view (b).

where n is the largest number of solvation molecules and m is the number of solvation molecules under the particular condition, C_1 and C_m are the concentration of solvent molecules corresponding to $m=1$ and $m=m$.

By applying this equation, we can estimate the number of solvated molecules at a given concentration of THF. Eq. (2) shows that C_m can be calculated by setting n and C_1. For example, in the case of $n=6$, $C_2=(10/4)C_1$, $C_3=(15/3)C_1$, $C_4=(20/2)C_1$, and so on. Therefore, we can obtain the calculated values for C_2, C_3, and C_4 by determining C_1. On the other hand, the shift for m solvated species (ΔE_m) can be obtained from the shift per one solvating THF molecule (ΔE_1) by $\Delta E_m = m\Delta E_1$. The solid line drawn in Fig. 3 shows the bathochromic shift of the emission band of TEA calculated according to Eq. (2). The calculations are carried out to obtain the best-fit agreement with experimental observations under the assumption that the maximum solvation number n equals to 6. The values of ΔE_1 and C_1 were set to be 1170 cm^{-1} and 0.82 mol dm^{-3}.

Fig. 5 shows the shift of the emission band of TOA in CH–THF mixtures. The agreement of the calculation with experimental observations is good. The calculation was done also by assuming $n=6$. The values of E_1 and C_1 were obtained as 1140 cm^{-1} and 0.72 mol dm^{-3}. These values for TOA are similar to those for TEA.

Fig. 6 shows the emission spectra of ABCO in CH–THF mixtures. Since almost half of the space around the N-atom of ABCO is shielded by the cage structure of alkyl groups, n for ABCO may be smaller than that for TEA and TOA (see

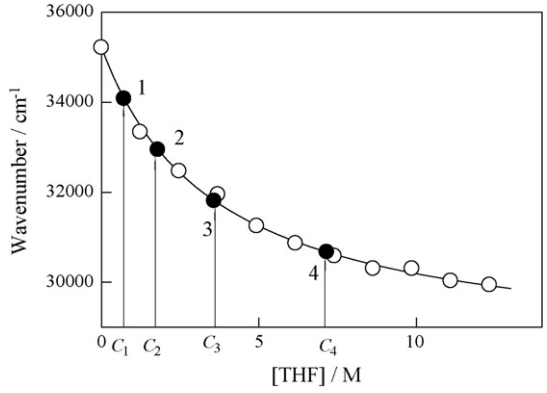

Fig. 5. The wavenumbers of the emission maxima of TOA against the concentration of THF in CH/THF mixtures: (◯) observed shifts; (●) calculated shifts from Eq. (2) (see text) (solvation numbers are shown along the curve).

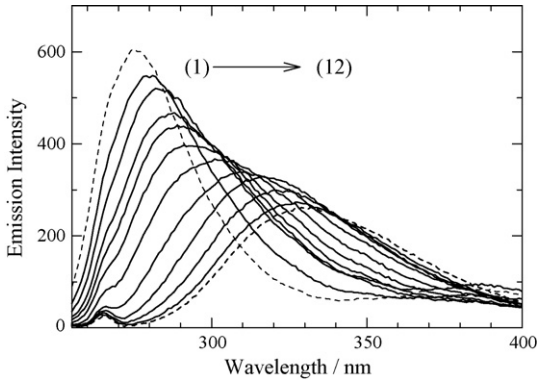

Fig. 6. Emission spectra of ABCO in CH/THF mixtures with different concentrations of THF. (1) [THF] = 0 mol dm^{-3}, (2) 0.31 mol dm^{-3}, (3) 0.62 mol dm^{-3}, (4) 0.92 mol dm^{-3}, (5) 1.23 mol dm^{-3}, (6) 1.54 mol dm^{-3}, (7) 2.16 mol dm^{-3}, (8) 3.70 mol dm^{-3}, (9) 6.17 mol dm^{-3}, (10) 8.63 mol dm^{-3}, (11) 11.10 mol dm^{-3} and (12) 12.33 mol dm^{-3}.

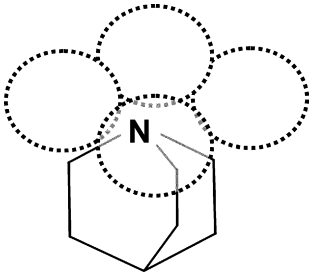

Fig. 7. A schematic model of solvated Rydberg state of ABCO. Polar solvent molecules are illustrated as cubes.

Fig. 7). The solid line in Fig. 8 shows the calculated values on the assumption of $n = 4$. As shown in Fig. 8, the agreement between calculated values and the observations is good. The values of E_1 and C_1 for ABCO are 1931 cm^{-1} and 1.23 mol dm^{-3}. These values are somewhat larger than those for TEA and TOA.

As shown above, the excited states of saturated amines are assigned as Rydberg states centered on the N-atom, and have quasicationic N-atom cores. In order to calculate the solvation energy for the present case, we used the following equation by considering the interaction between a cation and dipolar molecules

$$\Delta E_m = m\frac{ze\mu\cos\theta}{4\pi\varepsilon_0 r^2} \quad (3)$$

where m is the number of solvated molecule, ze the charge on the ion, μ the dipole moment of the solvent molecule, ε_0 the permittivity of vacuum, r the distance from the ion to the center of the dipole, and θ is the dipole angle relative to the line r joining the ion and the center of the dipole. ΔE_m corresponds to E_{op} in Eq. (1). The change of the $(E_{ex} - E_{ep})$ term with composition of THF in CH–THF mixtures was neglected, because the index of refraction of THF is similar to that of CH.

The value of $r = 0.59$ nm was obtained from the value of $\Delta E_1 = 1170$ cm^{-1} for TEA by assuming $\theta = 0°$ ($z = 1$ and $\mu = 5.80 \times 10^{-30}$ Cm for THF). In the case of $\theta = 0°$, the dipole is positioned next to the ion in such a way that the ion and the separated charges of the dipole are linearly arranged. The values of $r = 0.60$ and 0.46 nm were also obtained for TOA and ABCO. The smaller value for ABCO seems to reflect its compact structure.

Since only m and $m + 1$ solvated species are expected to exist between C_m and C_{m+1} in the successive solvation model shown above, the fraction of m solvated species can be estimated from the following equation (see Appendix B):

$$f_m = \frac{(m+1)(1 - C/C_{m+1})}{m(C/C_m - 1) + (m+1)(1 - C/C_{m+1})} \quad (4)$$

Figs. 9 and 10 show the changes in fractions of some solvated species for TEA and ABCO against the concentrations of THF, respectively. The fractions of higher solvated species increased with THF concentration. These figures visualize the stepwise solvation for TEA and ABCO.

The increase in medium polarity is also obtained by changing the density of the supercritical fluid of CHF_3. Fig. 11 shows the emission spectra of TEA in the gas phase and in several supercritical fluids with different densities of CHF_3. As shown in Fig. 11, the emission bands of TEA show a large red shift with increasing CHF_3 pressure.

As shown in Fig. 11, the shape of the emission spectra of TEF in CHF_3 supercritical fluid changed with CHF_3 pressure (the emission spectra of TEA at high pressures are unsym-

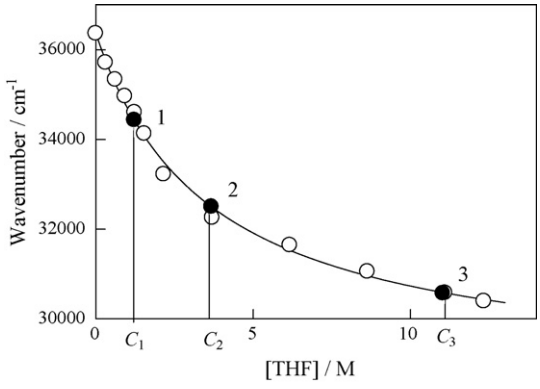

Fig. 8. The wavenumbers of the emission maximum of ABCO against the concentration of THF in CH/THF mixtures: (◯) observed shifts; (●) calculated shifts from Eq. (2) (see text) (solvation numbers are shown along the curve).

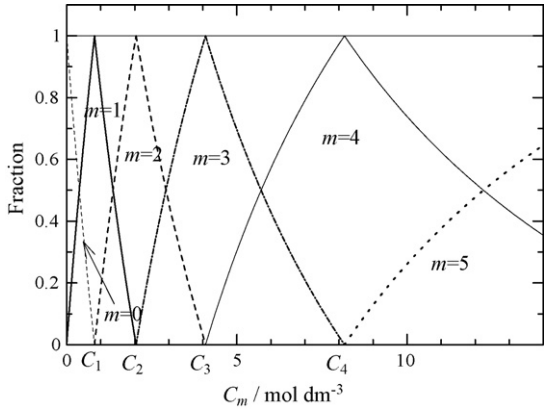

Fig. 9. Fraction of the species with different solvation numbers against the concentration of THF for TEA in CH/THF mixtures.

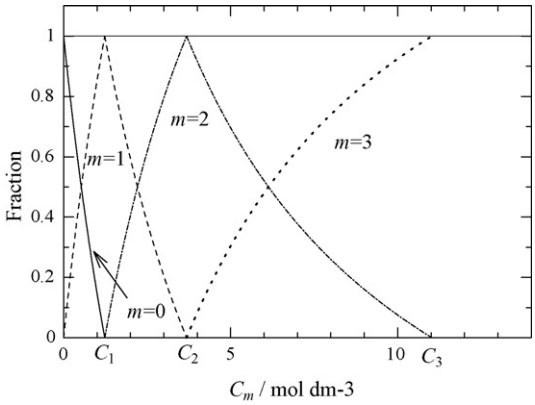

Fig. 10. Fraction of the species with different solvation numbers against the concentration of THF for ABCO in CH/THF mixtures.

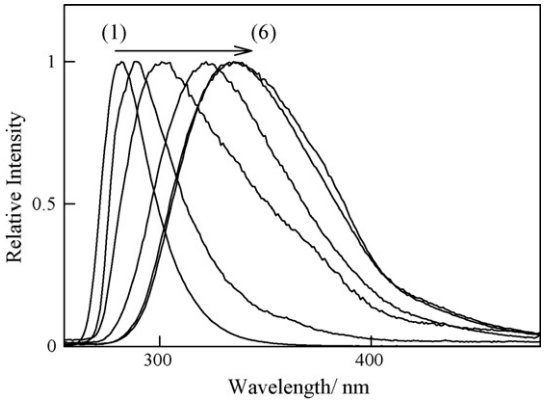

Fig. 11. Emission spectra of TEA in supercritical CFH_3 at different pressures. (1) $P(CHF_3) = 0$ bar, (2) 40.5 bar, (3) 50.7 bar, (4) 60.8 bar, (5) 70.9 bar and (6) 81.1 bar.

metrical). This indicates that the emission bands obtained at high pressures consist of two bands. Fig. 12 shows the separation of the emission band obtained at $P(CHF_3) = 50.7$ bar ($[CHF_3] = 5.6$ mol dm^{-3}) into two emission bands. The band appearing at short wavelengths is the original monomer band and the band at long wavelengths is attributed to the intermolecular excimer band. The relative intensity of the excimer band was found to increase with CHF_3 pressure. When the TEA sample

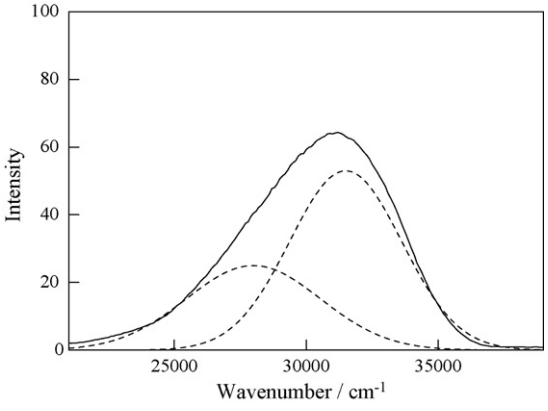

Fig. 12. Decomposition of the emission spectrum of TEA obtained for supercritical CFH_3 (at 50.7 bar) into two Gaussian curves.

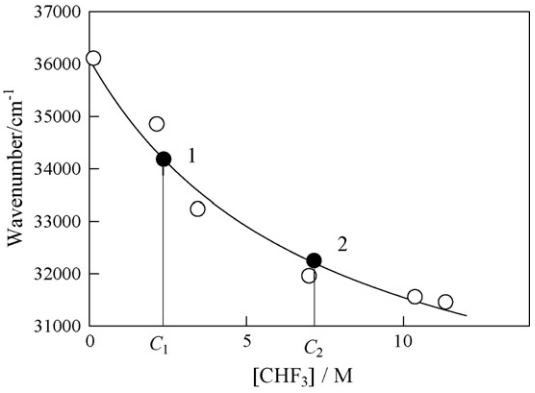

Fig. 13. The wavenumbers of the emission maximum of ABCO against the concentration of CFH_3 in the supercritical CFH_3: (◯) observed shifts; (●) calculated shifts from Eq. (2) (see text) (solvation numbers are shown along the curve).

was introduced into the cell, TEA adhered to the metal surface of the cell and it was solved to the CHF_3 fluid at high densities. Therefore, in the higher density fluids of CHF, the concentration of TEA was high enough to form the intermolecular excimer. Fig. 13 shows the shift of the monomer band of TEA with increasing CHF_3 concentration. The solid line shows the calculated value by assuming $n = 6$. The values of ΔE_1 and C_1 adopted for the best-fit curve were 1368 cm^{-1} and 2.66 mol dm^{-3}. As shown in Fig. 13, the agreement between the calculated values and the observations is good. The value of ΔE_1 for the TEA–CHF_3 system is similar to that for TEA–THF system, because the dipole moment of CHF_3 (5.50×10^{-30} Cm[12]) is very similar to that of THF. The C_1-value for CHF_3 supercritical fluids, however, is somewhat larger than that for CH–THF mixtures. In these cases, C_1 is expressed by $C_1 = k_{ds}/5k_s$, which can be obtained from Eq. (A.1). In the case of CHF_3 fluids, k_{ds} must be larger than that in the case of CH–THF mixtures, because the temperature is higher and the density around the solute molecule is smaller for the former case. On the other hand, the values of k_s are similar for both cases. These factors result in the larger value of C_1 and the smaller solvation number observed for the TEA–CHF_3 system compared with the TEA–THF

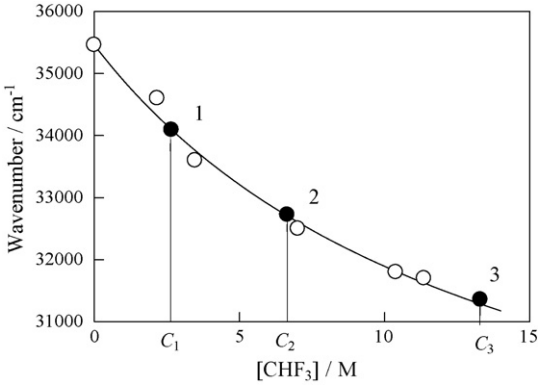

Fig. 14. The wavenumbers of the emission maxima of ABCO against the concentration of CFH_3 in the supercritical CFH_3: (◯) observed shifts; (●) calculated shifts from Eq. (2) (see text) (solvation numbers are shown along the curve).

system in a similar concentration regime of polar solvent molecules.

Fig. 14 shows the shift of the emission band of ABCO with increasing CHF_3 concentration. The solid line shows the calculated values on the assumption of $n=4$. As shown in Fig. 14, the agreement between the calculated values and the observations is good. The values of ΔE_1 and C_1 adopted for the best-fit curve were $1930\,cm^{-1}$ and $2.39\,mol\,dm^{-3}$. The similar tendencies mentioned above for the TEA–CHF_3 system are also observed for the ABCO–CHF_3 system. The values of r for TEA and ABCO in CHF_3 fluid could not be estimated, because the change in the $(E_{ex}-E_{ep})$ term with the concentration of CHF_3 seems to be nonnegligible in this case.

4. Conclusion

The large successive red shifts of emission bands of some tertiary amines were observed by increasing concentrations of polar solvent molecules in CH–THF mixtures and CHF_3 supercritical fluids. These shifts were explained by a consecutive solvation model. The changes in the fraction of each solvated species were depicted as a function of the concentration of THF.

Appendix A

The rates of the desolvation and solvation are represented by $k_{ds}m$ and $k_s(n-m)C$, where m and n are the number of polar solvent molecules accommodated at solvation sites at the concentration of polar solvent (C) and its maximum number, and k_{ds} and k_s are rate constants for desolvation and solvation. At equilibrium, these two rates should be equal and hence

$$k_{ds}m = k_s(n-m)C_m \tag{A.1}$$

This equation is also satisfied when $m=1$ and $C=C_1$. Using this condition, we can obtain the following equation:

$$C_m = C_1\frac{m(n-1)}{n-m} \tag{A.2}$$

Appendix B

For equilibrium at C between C_m and C_{m+1}, the following equation was obtained under the assumption that only m and $m+1$ solvated species exist between C_m and C_{m+1}:

$$f_m k_{ds}m + (1-f_m)k_{ds}(m+1) = f_m k_s(n-m)C + (1-f_m)k_s(n-(m+1))C \tag{B.1}$$

where f_m is the fraction of m solvated species between C_m and C_{m+1}. At C_m and C_{m+1}, the following equations of course hold:

$$k_{ds}m = k_s(n-m)C_m \tag{B.2}$$

$$k_{ds}(m+1) = k_s(n-(m+1))C_{m+1} \tag{B.3}$$

Using these equations, we could obtain the following equation for f_m:

$$f_m = \frac{(m+1)(1-C/C_{m+1})}{m(C/C_m-1)+(m+1)(1-C/C_{m+1})} \tag{B.3}$$

In a similar manner, the fraction of nonsolvated species (f_0) between 0 and C_1 was obtained.

$$f_0 = \frac{(n-1)(C_1-C)}{(n-1)C_1+C} \tag{B.4}$$

References

[1] A.M. Halpern, Chem. Phys. Lett. 6 (1970) 296.
[2] C.G. Freeman, M.J. McEwan, R.G.F.C. Clarridge, L.F. Philips, Chem. Phys. Lett. 8 (1971) 77.
[3] A.M. Halpern, T. Gartman, J. Am. Chem. Soc. 96 (1974) 1393.
[4] A.M. Halpern, A.L. Lyons Jr., J. Am. Chem. Soc. 98 (1976) 416.
[5] A.M. Halpern, D.K. Wong, Chem. Phys. Lett. 37 (1976) 416.
[6] M.B. Robin, Higher Excited States of Polyatomic Molecules, vol. 1, Academic Press, New York, 1974, p. 268.
[7] P. Avouris, A.R. Rossi, J. Phys. Chem. 85 (1981) 2340.
[8] Y. Muto, Y. Nakato, H. Tsubomura, Chem. Phys. Lett. 9 (1971) 597.
[9] M.B. Robin, Higher Excited States of Polyatomic Molecules, vol. 1, Academic Press, New York, 1974, p. 23.
[10] M. van der Auweraer, F.C. De Schryver, A. Gilbert, S. Wilson, Bull. Soc. Chim. Belg. 88 (1979) 227.
[11] A.M. Halpern, J. Phys. Chem. 85 (1981) 1682.
[12] A.M. Halpern, R.M. Danzinger, Chem. Phys. Lett. 16 (1972) 72.
[13] A.M. Halpern, J. Am. Chem. Soc. 97 (1975) 2971.
[14] A.M. Halpern, M.W. Legenza, B.R. Ramachandran, J. Am. Chem. Soc. 101 (1979) 5736.
[15] S. Yamamoto, H. Habara, Chem. Lett. (1997) 757.
[16] S. Yamamoto, H. Habara, Y. Sueishi, Phys. Chem. Chem. Phys. 1 (1999) 421.
[17] G. Kohler, J. Photochem. 35 (1986) 189.
[18] G. Kohler, J. Photochem. Photobiol. A Chem. 40 (1987) 307.
[19] G. Kohler, J. Phys. Chem. 91 (1987) 2051.
[20] Q.Y. Shang, P.O. Moreno, E.R. Bernstein, J. Am. Chem. Soc. 116 (1994) 311.
[21] Y.C. Hou, J.J. Martin, AIchE J. 5 (1959) 125.
[22] O. Kajimoto, M. Futakami, T. Kobayashi, K. Yamasaki, J. Phys. Chem. 92 (1988) 1347.
[23] A. Morita, O. Kajimoto, J. Phys. Chem. 94 (1990) 6420.